International Journal of Nanoelectronics and Materials
IJNeaM
ISSN 1985-5761 | E-ISSN 2232-1535

Testing aluminium and polytetrafluoroethylene as triboelectric materials for acoustic triboelectric nanogenerators

Muhammad Idzuan Bin Zambri[a], Irfan Bin Abdul Rahim[a,b,c]*, Zarhamdy Bin Md Zain[d], Mohd Sazli Bin Saad[a], Mohammad Faridun Naim Bin Tajuddin[c,e], Ahmad Hamdan Bin Ariffin[b,f], and Irna Farikhah[g]

[a]*Faculty of Mechanical Engineering Technology, Universiti Malaysia Perlis Kampus Tetap Pauh Putra, 02600 Arau, Perlis, Malaysia*
[b]*Green Design and Manufacture Research Group, Center of Excellence Geopolymer and Green Technology (CEGeoGTech), Universiti Malaysia Perlis, 01000 Kangar, Perlis, Malaysia*
[c]*Center of Excellence for Renewable Energy (CERE), Faculty of Electrical Engineering & Technology, Universiti Malaysia Perlis (UniMAP), 02600 Arau, Perlis, Malaysia*
[d]*Faculty of Mechanical Engineering, Universiti Teknologi Malaysia, 81310 Skudai, Johor Bahru, Johor, Malaysia*
[e]*Faculty of Electrical Engineering & Technology, Universiti Malaysia Perlis, 02600 Arau, Perlis, Malaysia*
[f]*Faculty of Mechanical and Manufacturing Engineering, Universiti Tun Hussein Onn Malaysia, 86400 Batu Pahat, Malaysia*
[g]*Department of Mechanical Engineering, Faculty of Engineering and Informatics, Universitas PGRI Semarang, Semarang 50232 Indonesia*
** Corresponding author. e-mail: irfanrahim@unimap.edu.my*

Received 14 July 2025, Revised 8 October 2025, Accepted 21 October 2025

ABSTRACT

Triboelectric Nanogenerator (TENG) is a green energy generating technology that can harvest energy from the surroundings such as ambient sound via contact-electrification and triboelectric effects. TENG works by exchanging electrons through different triboelectric materials to generate current flow. Polytetrafluoroethylene (PTFE) and Aluminium were selected to be the triboelectric materials of an Acoustic TENG due to their good flexibility, lightweight, low cost, recyclability and great affinities of the materials to a accept and donate electrons. A conventional speaker enclosed in an acrylic chamber was used to simulate the sinusoidal soundwave of the TAE. The TENG was tested with different sound frequencies to determine the optimum frequency for the electrical output of the system. The TENG can produce maximum and minimum open-circuit voltage of 2.36V and -2.76V at the sound frequency of 60Hz. At this frequency, the TENG can also generate 0.206 μW using 7 MΩ load resistance. The triboelectric pair of PTFE-Al generated significantly lower electrical output when compared to other PTFE-Al based TENG in scientific literature. The unexpected low output of this study's TENG may occur due to poor contact and separation process between the active and the static layers of the TENG in this study. Further improvements need to be made to the design of the TENG to ensure proper separation of the triboelectric layers during the energy conversion process.

Keywords: *Acoustic triboelectric nanogenerator, Triboelectric materials, PTFE, Aluminium, Frequency, Open-Circuit voltage, power*

1. INTRODUCTION

Triboelectric Nanogenerator or (TENG) is an emerging technology that uses triboelectric materials to convert mechanical energy into electrical energy [1,2]. It functions by combining contact-electrification and triboelectric effects where triboelectric charges at two materials are exchanged or transferred after the materials have been separated from physical contact [3-6]. The TENGs are ideal at harvesting energy from the environment because they are most effective at converting irregular, low-amplitude and low frequency mechanical energy into electricity [7]. Recent studies show that the TENG can be applied in wearable applications [8-10], biological sensors [11-13], self-powered sensor systems [14-16] and blue energy/ waves harvesting [17-19].

Ambient sound can also be the source of mechanical energy which can be harvested by TENGs [20]. These TENGs are called Acoustic Triboelectric Nanogenerators (A-TENG). Choosing triboelectric materials for an A-TENG is crucial for efficiently converting acoustic vibration into electricity [21]. Different triboelectric materials had been used to enhance the surface charges and electrical output from an A-TENG [22]. Materials such as graphene which exhibit good electrical property, flexible, have high surface-to-volume ratio as well as great malleability due to its low atomic thickness, are a leading candidate for the active materials in A-TENGs and in conventional TENG [23,24].

Recent advancement in nanostructures and nanocomposites can also enhance the electrical output of the TENGs [25-29]. These advancements have helped to create TENGs that are lightweight and more efficient as well as increasing their durability and compatibility to complex environment [30]. For example, an A-TENG called Integrated Acoustic Metamaterial Triboelectric Nanogenerator (IAM-TENG) that integrates multi-walled carbon nanotube (MWCNTs) and Fluorinated Ethylene Propylene (FEP) membrane as its triboelectric layers, was able to generate 0.93 mW of power when operated at its optimal frequency and at acoustic excitation of 100 dB [31].

Polymers is also a popular choice to be the triboelectric materials for a triboelectric nanogenerator due to its lightweight, malleability, durability and anti-microbial features [32]. Advancement in manufacturing of Porous Polymer Materials (PPMs) made from hydrogels, aerogels, foams and fibrous media with different geometries and topologies has also been utilized to improve the performance of TENGs [33]. Furthermore, Biodegradable TENG (BD-TENG) using biodegradable polymers becomes an emerging energy harvesting device with the benefits of reducing pollution to the environment [34]. For acoustic TENGs specifically, polymers such as porous Polyvinylidene fluoride (PVDF), Polyethylene terephthalate (PET), and Polydimethylsiloxane (PDMS) are often used due to their compatibility and sensitivity to soundwaves [20].

Thus, there is no shortage of materials to be chosen as the triboelectric materials in a TENG. These triboelectric materials have undergone some kind of mechanical and chemical doping process which can greatly improve the performance of the TENG [35]. However, the doping processes come with its own set of challenges and can introduce complications in the manufacturing process as well as relatively costly to implement in a bigger scale [36].

Hence, the study aims to implement two simple triboelectric materials that are widely available to be implemented in an acoustic TENG. The results of this study may become a measuring stick or a reference point for future research on triboelectric materials in a TENG.

2. WORKING PRINCIPLE OF TRIBOELECTRIC NANOGENERATOR

One of the simplest types of TENG is a contact-separation mode consisting of two electrodes (metal conductor) and two dielectrics (polymers) [1]. The contact-separation mode TENG is depicted in **Figure 1**.

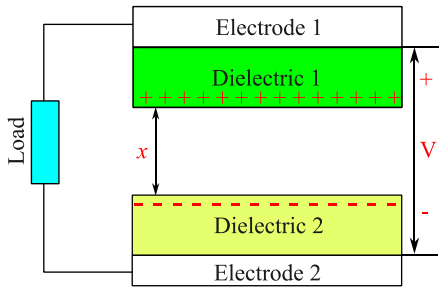

Figure 1. Contact-separation mode TENG consists of electrodes and dielectrics that is connected to a load

The electrodes and dielectrics form a pair of triboelectric materials named tribo-pairs. The electrode is usually made from metal conductor while the dielectrics is often made of polymers. When an alternating mechanical force is applied to the two triboelectric layers, the distance between the layers, x can be changed. If the distance between the tribo-layers keep changing, a potential difference, V will be induced due to the electric field generated from the flow of triboelectric charges between both triboelectric layers [37]. This process of electrical generation can be mathematically modelled using key equations [30]. According to these key equations, the potential difference, V can be expressed as below:

$$V = -\frac{Q}{C(x)} + V_{oc}(x) \quad (1)$$

Where Q is the charge transfer between the dielectric layers, C is the capacitance of the dielectric layers, x is the distance between the two dielectric layer and V_{oc} is open circuit voltage of the TENG. The open-circuit voltage generated by the TENG follows the following governing equation:

$$V_{OC} = \frac{\sigma\, x(t)}{\varepsilon_0} \quad (2)$$

Where ε_0 is the free space permittivity constant, $x(t)$ is the separation distance between the two TENG layers, and σ is the surface charge density.

Capacitance, C from equation (1) can be defined as:

$$C = -\frac{S\varepsilon_0}{d_0 + x(t)} \quad (3)$$

Where S is the surface contact area of the dielectric material, ε_0 is the free space permittivity which is $8.8541878188 \times 10^{-12}$ Fm^{-1}, $x(t)$ is the separation distance between the two TENG layers. The effective thickness, d_0 is described as the summation of all thickness of the dielectric, t_i divided by their relative dielectric constant, ε_{ri}:

$$d_0 = \sum_{i=1}^{n} \frac{t_i}{\varepsilon_{ri}} \quad (4)$$

By combining Equation (1) with Equations (2) and (3), The total voltage from the two electrodes in **Figure 1** can be further described as:

$$V = -\frac{Q}{S\varepsilon_0}\big(d_0 + x(t)\big) + \frac{\sigma x(t)}{\varepsilon_0} \quad (5)$$

2.1. Working Principle of Acoustic Triboelectric Nanogenerator

In an A-TENG, triboelectric layers can be divided into the active and the static layer. The active layer acts as a diaphragm that flexes due to acoustic pressure wave (soundwave) from the surrounding while the static layer remain stationary. The flexing of the active layer changes the separation distance, x. The changes of x will cause the triboelectric charge in the TENG's layer to be exchanged between the active and static layers, generating currents and potential difference in the process. This process is illustrated in **Figure 2**.

From **Figure 2**, before contact, no charge is transferred from the one active layer to the other static layer. Thus, no electric potential is generated between the layers. When acoustic waves reach the active layer, the active layer flexes towards the passive layer. The changes in separation distance creates electric potential which causes triboelectric charge in the passive layer to flow into the active layer until the two layers are in contact. When both layers are in contact, the total negative and positive charge

in both layers is equal resulting in no charge flow between them. Due to the elasticity of the active layer and the acoustic wave, the active layer will then flex away from the passive layer, generating an electric field. This causes the triboelectric charges to flow from the active layer into the passive layer or in the opposite direction from before. The flow stops until the active layer is at the maximum separation. Then, the active layer flexes towards the static layer again, repeating the entire cycle of alternating charge flow [38].

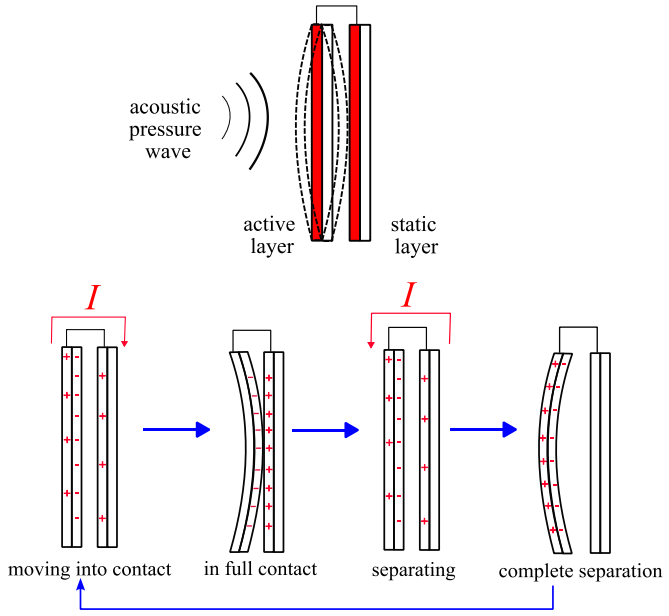

Figure 2. working principle of the acoustic TENG

3. METHODOLOGY

3.1. Selecting the Triboelectric Materials for the Acoustic TENG

Since TENGs generate electricity through contact-electrification and triboelectric effects, selecting materials for any TENGs must be based on the triboelectric series [39]. This is because triboelectrification is electron transfer between two materials in physical contact. The direction of the electron transfer depends on the difference in the electron affinities of the two materials. Higher electron affinities material will attract electron from the other. This material becomes the electron acceptor. The material that loses electrons is consequently become the electron donor. The affinities of the materials can generally be identified by their order in the triboelectric series. The first triboelectric series was published in 1757 by Johan Carl Wilcke [40]. However recently in 2019, a more reliable triboelectric series was built that quantifies the triboelectric charge density of different materials based on their triboelectrification with mercury when operating in contact-separation mode [41].

Furthermore, when selecting triboelectric materials for a TENG, the materials must have high charge density and high durability. High charge density materials allow for better output performance from the TENGs while high durability materials create more stable and long-lasting TENGs [7]. For an acoustic TENGs specifically, the materials especially the active layer in **Figure 2** must be flexible enough to harvest the energy from the acoustic wave [42]. One more consideration that is applied in this study is that the materials must be relatively low cost to be purchased and widely available within the commercial industry.

Based on these considerations, Polytetrafluoroethylene (PTFE) was chosen to be the electron acceptor and the dielectric materials while Aluminium (Al) was picked as the electron donor for the acoustic TENG.

PTFE is one of the most popular choices as the electron acceptor because it is always one of the strongest electron acceptors due to the strong electron attractive force of fluorine element in PTFE [39,43]. Additionally, polymer materials have other traits such as great flexibility, machinability, low weight and scalability. [32-34,43]. Moreover, PTFE has large affinities for accepting electrons and possess high surface charge density according to the new triboelectric series from Zou [41]. The same triboelectric series also shows that PTFE has more charge densities than other popular polymer that is used in TENGS such as Polydimethylsiloxane (PDMS), Fluorinated ethylene propylene (FEP) and Polyvinylidene fluoride (PVDF) [43]. Higher charge density allows for more surface charge to flow during the energy generation process of the TENGs. More importantly, PTFE strips can also be purchased off the shelve in commercial market and are low cost.

Aluminium (Al) is chosen because it can both act as an electron donor and as an electrode for the TENG. Aluminium foil or film are widely available, recyclable, low cost and had been implemented with polymers in many TENGs [44-46]. Furthermore, when aluminium is paired with PTFE, it can generate more potential difference according to the triboelectric series when compared to other conductive metal such as copper and steel [47-50].

3.2. Fabrication of the Acoustic TENG

The acoustic TENG made from PTFE-Al pairs was divided into two sides. One side serves as the active layers which acts as a diaphragm that's flexes and vibrate from the incoming acoustic wave while the other acts as the static layers. Each triboelectric material is 0.5 mm thick and were cut into a circle with 80 mm diameter as shown in **Figure 3**. The configuration of PTFE and Al films for the TENGs was depicted in **Figure 4**. **Figure 4** also shows that x is the separation distance for the triboelectric layers of the TENG.

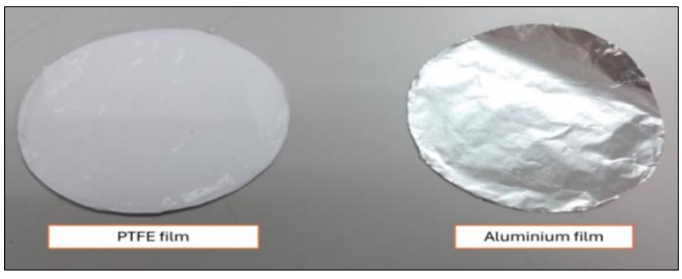

Figure 3. PTFE film and Aluminium film/foil were 0.5 mm thick and cut with diameter of 80 mm to be used in the TENG

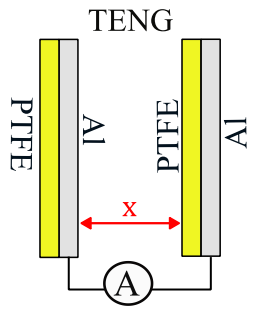

Figure 4. The PTFE and Al films was arranged in this configuration when used as the dielectric pairs for the TENG

3.3. Acoustic Test on the TENG

An experimental setup was made according to the schematic diagram shown in **Figure 5** to test the performance of the acoustic TENG in varying operating frequencies. A function generator (model type: MFG-8255A) provides a sinusoidal wave signal starting from the frequency of 10 Hz to 500 Hz for the loudspeaker. A conventional 6.5-inch loudspeaker (L.A. Power model LA-621 with peak power of 380W) acts as the acoustic driver, generating the acoustic wave to the TENG. The speaker is enclosed in a chamber made from transparent acrylics with the dimension of 169 mm × 169 mm × 169 mm. The acrylic chamber ensures that no sound coming from the speaker escapes to the surroundings and helps redirect the sound into the acoustic tube. Moreover, the speaker was connected to an acoustic tube which is made from a combination of PVC pipe fittings and a 3D printed PLA polymer. The 13.5 cm acoustic tube is tapered from a 16.51 cm (6.5-inch) diameter to a 3.8 cm diameter in the middle which then widened to a 6 cm diameter at the other end. The TENG was then mounted to the end of the acoustic tube. The TENG harvested the mechanical acoustic energy provided by the speaker and converted the mechanical energy into electrical energy. An ATTEN ADS1062 Digital Oscilloscope was connected to two electrodes (Al) of the TENG to measure the open circuit voltage generated from the TENG. **Figure 6** shows the enclosed loudspeaker and the acoustic tube connected to the TENG.

Figure 7 shows setup of the acoustic experiment. From **Figure 7**, The function generator provided sinusoidal electric signal to the loudspeaker. The loudspeaker then converted this electric signal into the corresponding sinusoidal acoustic wave. The TENG was subjected to sinusoidal acoustic waves ranging from 10 Hz to 100 Hz with 10 Hz intervals from the loudspeaker. The open circuit voltage generated by TENG due to the mechanical vibration of the soundwave was then measured by the digital oscilloscope at 0.08 ms interval for 1 s. This frequency range was purposely selected to determine the practicality of the acoustic TENG when operating at a low operating frequency as predicted in [30]. Results for the effect of the frequency of the soundwave on the output open-circuit voltage were collected and processed for analysis. The experiment was then repeated with different ranges of frequency beginning from 100 Hz to 500 Hz with 100 Hz intervals to determine the best operating frequency for the TENG. The TENG was then connected to an external load resistor to generate power. The power generated by the load was measured using the value of input sound frequency that can generate the highest open-circuit voltage

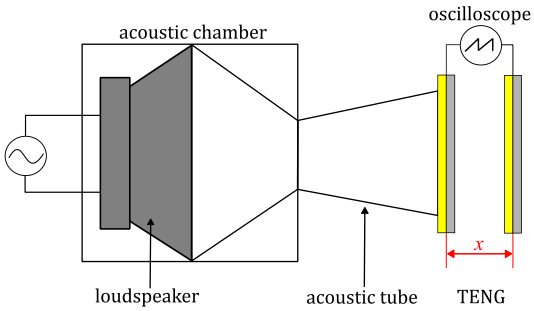

Figure 5. Schematic diagram of the experimental setup

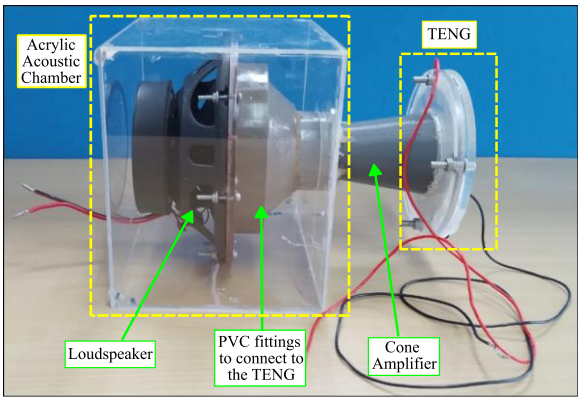

Figure 6. Photograph of the enclosed speaker connected to the TENG

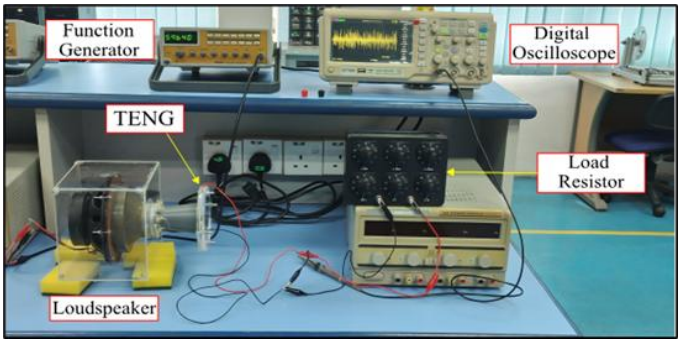

Figure 7. Photograph of the Experiment Setup

4. RESULTS OF THE ACOUSTIC TEST

4.1. Open-Circuit Voltage Analysis

The result from the acoustic test shows that the triboelectric pairs of PTFE and Aluminium manage to generate an open circuit voltage during the experiment. This means that the triboelectric pair can become a viable triboelectric material for an acoustic TENG. The TENG's triboelectric layers were able to convert the sinusoidal acoustic wave from the speaker into an electrical output. The effect of the frequency of the soundwave on the electric generation is studied by plotting the maximum and minimum open circuit voltage, V_{OC} produced by the TENG is shown in **Figure 8**. From **Figure 8**, the V_{OC} generated from the TENG fluctuates when the frequency is lower than 100 Hz. Then, the V_{OC} remains relatively constant beyond the frequency of 100 Hz. The current result shows that the PTFE and Aluminium layer is

not able to generate more V_{OC} at frequency higher than 100 -Hz which suggests that the acoustic TENG in this study is more suitable for operating in sound frequency lower than 100 Hz. At sound frequency of 60 Hz, the maximum and minimum V_{OC} of 2.36 V and -2.76V respectively were generated by the acoustic TENG.

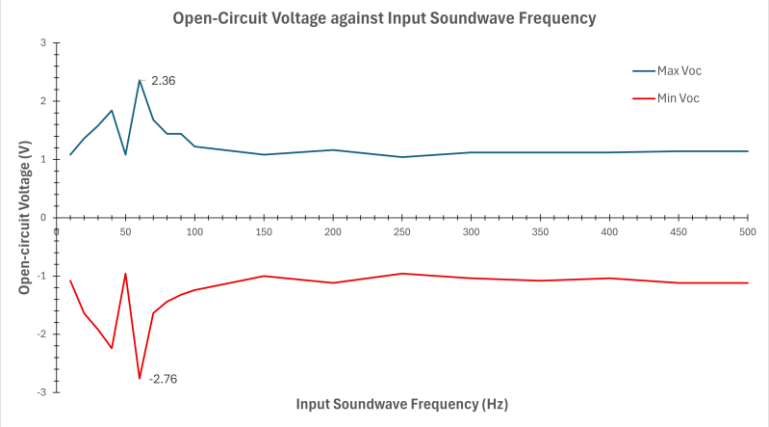

Figure 8. The maximum and minimum open circuit voltage produced by the acoustic TENG.

Similar PTFE-Al based TENG from other studies managed to generate significantly higher open-circuit voltage than the TENG in this study [44,51]. These PTFE-Al TENGs were aided with other factors to improve their performance. One of these aiding factors was Graphene. Graphene had been shown to enhance the power densities of the triboelectric materials, thus, increasing the power output and the efficiency of the TENG [23,28,51,52]. However, Graphene also significantly increases the production and manufacturing cost of the TENG. The TENG used in this study is more cost-effective because all materials used are simple materials that can be easily procured from its relevant commercial space.

A new design for the PTFE-Al using the "air-breakdown module" where aluminium electrode was made with crumpled aluminium foils was able to generate better charge transfer [51]. However, this design is ill-suited for acoustic energy harvesting and require constant high force input to generate good energy outcome from the TENGs.

There was a study that produced similar output when compared to this works' PTFE-Al TENG [53]. The study used a free-standing mode TENG and was fabricated to be used in high-temperature environment. Although, the TENGs managed to generate significant open-circuit voltage at high-temperature, the TENG needs constant cooling from its' water-based cooling system. The constant cooling condition limits the energy production of the TENG. **Table 1** summarizes the significant differences of this study of TENG with other similar PTFE-Al based TENG in the scientific literatures.

The unexpected low output from this study's PTFE-Al TENG may also occur because of the poor contact and separation between the active and the static layers of the TENG in the experiment which could severely reduce the generation of V_{OC}. **Figure 9** shows the actual contact and separation process of the triboelectric layers during the acoustic frequency test. During the test, it was observed that the triboelectric layers of the TENG stuck and oscillated together instead of separating after the initial contact of the active layer with the static layer. Since the triboelectric layer could not separate properly as illustrated in **Figure 2**, no charge imbalance exists. If there is no charge imbalance, no charge flow will occur during the process. Hence, no current is generated, and no potential difference is produced.

Table 1 . Significant differences between the PTFE-Al TENG from this study and from other relevant studies

Research	**Dielectric materials in TENGs**	**Open-Circuit Voltage generated, V_{OC} (V)**	**Novelty/Significant of Research**
(F. Ali et al. 2022)[44]	Plastic Waste Bottle (PTFE), Aluminium Foil, Graphene	1400 V	The presence of Graphene greatly enhanced V_{OC}.
(Son et al. 2023) [51]	PTFE, Aluminium (electrodes), and crumpled aluminium	648 V	Crumpled aluminium foil combined with air-breakdown model were used for charge transfer between the aluminium electrode and PTFE layers

	foil (charge transfer medium)		
(Shoumik et al. 2024)[53]	PTFE and Aluminium	0.832	Free standing mode TENG was designed using PTFE and Al foils to be used in high-temperature environment
This work	PTFE and aluminium	2.36	Simple TENG that was designed to harvest acoustic energy using readily available and recyclable materials

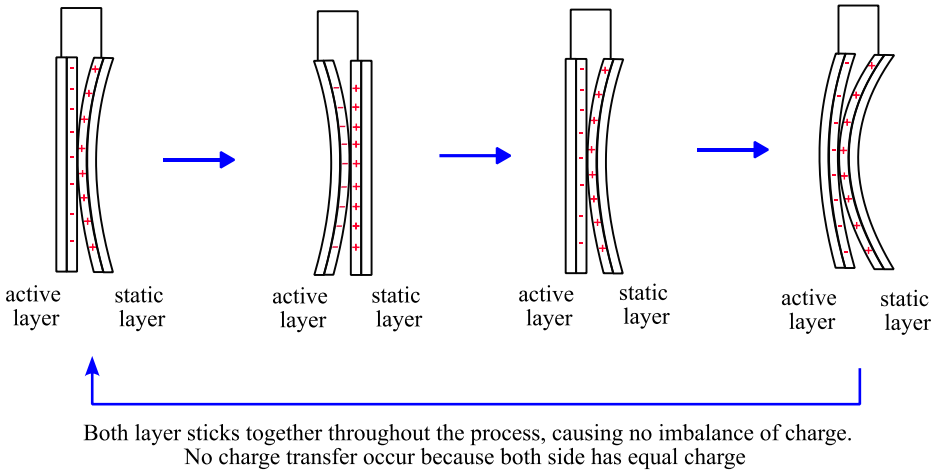

Figure 9. The observed movement of the triboelectric layers during the acoustic test

The study hypothesised that improper separation of the triboelectric layers is perhaps caused due to high friction between the static PTFE layer and the active Aluminium layer. It has been reported that when selecting triboelectric materials for a TENG, the materials must have friction coefficient, μ that is lower than the threshold value of μ_{th}, which is estimated to be around 0.4 to reduce wear and heat during friction process [54]. The friction coefficient, μ of aluminium to PTFE maybe higher than the μ_{th} which may cause strong adhesion between the materials. Observation from other study also shows that when a PTFE pin was slid onto an aluminium disc, the materials have strong adhesion possibly because of the formation of carbon-metal bonds [55]. Thus, due to the strong adhesion between PTFE and aluminium, the materials may have not separated properly after contact.

Further test needs to be conducted to verify that adhesion is the main contributor to the poor performance of the TENG. A high-speed camera could be used to observe the oscillation of the active layer the acoustic energy harvesting process to have a more comprehensive understanding of the adhesion of the PTFE and Aluminium layer. Moreover, the design of the TENG can be modified by adding an intermediate layer that can reduce the friction and mitigate the adhesion between the dielectric PTFE layers and the Aluminium electrodes.

4.2. Resistive Loading Analysis

Figure 10 shows that the voltage across the resistor increases rapidly at around 1 MΩ until it reaches a peak of 1.84 V at 70 MΩ. The root-mean-square (RMS) voltage then decreases slightly to 1.6 V at 100 MΩ and continue to increase to 1.92 V at 1 GΩ. The smallest value of the current is 1.92 nA at the highest load resistance of 1 GΩ while the highest current is 0.43 μA at the lowest load resistance of 10 kΩ.

In general, the output voltage of a TENG increases as load resistance increases while the current output shows the opposite trend [56]. As reported in a published work in [57], a load in TENG exhibited three characteristics during resistive loading. In the first region, while the resistance is relatively small, the load is in Constant Current - Output Characteristic Region (CC-OCR). During CC-OCR, the current that passes through the load will be large and relatively constant while the voltage increases linearly. As the resistance of the load increases, the load will enter the Maximum Power – Output Characteristic Region (MP-OCR) where the load voltage rapidly increases while the current quickly decreases. In this region, the maximum power generated by the load can be identified. By further increasing the load resistance, the load enters the Constant Voltage – Output Characteristic Region (CV-OCR) where the voltage approaches the value of the open-circuit voltage and stays almost constant, while the currents continue to decrease slowly.

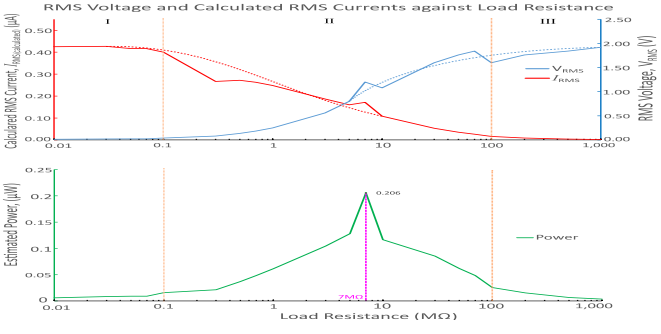

Figure 10. The voltage, current and instantaneous power generated from the load resistor

The results from **Figure 10** also showed that the TENG generated the highest instantaneous power of 0.206 μW at 7 MΩ load resistance. This means that the TENG's operating load resistance is at 7 MΩ because it can produce the highest power at this load. At this small power output, the TENG could power small electronic and portable devices such as LEDs as shown in other similar studies [44,53]. However, PTFE and Aluminium pairing provide a good starting base for the selection of the triboelectric pairs for an acoustic TENG.

Further improvement to the design of the TENG such as introducing an intermediate layer that reduces friction of the PTFE-Al layers could be implemented to increase the power generated by the PTFE-Al based TENG. Moreover, by introducing another triboelectric material to the PTFE-Al pair could potentially increase the performance of the TENG as well [28,44].

5. CONCLUSION

This study proposes PTFE and Aluminium as the triboelectric materials for an Acoustic TENG that can harvest and transform the mechanical energy from acoustic waves into useful electricity. PTFE was selected because it has great flexibility, machinability, scalability, low weight as well as large affinities for accepting electrons and possess high surface charge densities [32-34,41,43]. Aluminium was chosen because it can be both as an electron donor and as an electrode for the TENG. Aluminium foil or film are widely available, recyclable, and low cost [44-46]. When paired with PTFE, aluminium can generate more potential difference compared to other widely used metal such as copper and steel [47-50]. The study shows that the TENG can generate more open circuit voltage within the low frequency region of 10-100 Hz with the maximum and the minimum open-circuit voltages of 2.36 V and -2.76 V occurring at 60 Hz. The Acoustic TENG generated 0.206 μW at 7 MΩ load resistance. The open circuit voltage generated by the TENG is much lower than anticipated when compared to other similar studies [44,51]. The lower output of the TENG may occur possibly due to improper contact and separation of the TENG layers that perhaps severely decreased the open-circuit voltage generated by the TENG. Hence, to reduce the adhesion effect of the two layers in the TENG, the design of the acoustic TENG can be modified by implementing an intermediate layer between the active and passive layer or by testing other alternative electrodes. Furthermore, introducing more triboelectric materials such as Graphene, PDMS and PVDF to create a hybrid pairing to the PTFE-Al pairs could increase the electrical productivity of the TENG.

ACKNOWLEDGMENTS

The research is supported by Universiti Malaysia Perlis Grant, 9001-00772: Geran Pascasiswazah 2023 (Sains & Teknologi). The authors also acknowledge support from Universiti Malaysia Perlis for providing the facilities used in this study.

REFERENCES

[1] W. G. Kim, D. W. Kim, I. W. Tcho, J. K. Kim, M. S. Kim, and Y. K. Choi, 'Triboelectric Nanogenerator: Structure, Mechanism, and Applications', Jan. 26, 2021, American Chemical Society. doi: 10.1021/acsnano.0c09803.

[2] C. Wu, A. C. Wang, W. Ding, H. Guo, and Z. L. Wang, 'Triboelectric Nanogenerator: A Foundation of the Energy for the New Era', Jan. 03, 2019, Wiley-VCH Verlag. doi: 10.1002/aenm.201802906.

[3] S. Niu and Z. L. Wang, 'Theoretical systems of triboelectric nanogenerators', Nano Energy, vol. 14, pp. 161–192, Oct. 2014, doi: 10.1016/j.nanoen.2014.11.034.

[4] Z. L. Wang, L. Lin, J. Chen, S. Niu, and Y. Zi, 'Triboelectric Nanogenerator: Vertical Contact-Separation Mode', 2016, pp. 23–47. doi: 10.1007/978-3-319-40039-6_2.

[5] J. Shao, M. Willatzen, and Z. L. Wang, 'Theoretical modeling of triboelectric nanogenerators (TENGs)', J Appl Phys, vol. 128, no. 11, Sep. 2020, doi: 10.1063/5.0020961.

[6] H. Zhao et al., 'Theoretical modeling of contact-separation mode triboelectric nanogenerators from initial charge distribution', Energy Environ Sci, vol. 17, no. 6, pp. 2228–2247, Feb. 2024, doi: 10.1039/d3ee04143c.

[7] T. Cheng, J. Shao, and Z. L. Wang, 'Triboelectric nanogenerators', Nature Reviews Methods Primers, vol. 3, no. 1, Dec. 2023, doi: 10.1038/s43586-023-00220-3.

[8] V. Vivekananthan, A. Chandrasekhar, N. Rao Alluri, Y. Purusothaman, G. Khandelwal, and S.-J. Kim, 'Triboelectric Nanogenerators: Design, Fabrication, Energy Harvesting, and Portable-Wearable Applications', in Nanogenerators, Sang-Jae Kim, Arunkumar Chandrasekhar, and Nagamalleswara Rao Alluri, Eds., 2020. [Online]. Available: www.intechopen.com

[9] H. Chu, H. Jang, Y. Lee, Y. Chae, and J. H. Ahn, 'Conformal, graphene-based triboelectric nanogenerator for self-powered wearable electronics', Nano Energy, vol. 27, pp. 298–305, Sep. 2016, doi: 10.1016/j.nanoen.2016.07.009.

[10] H. Zheng et al., 'Concurrent Harvesting of Ambient Energy by Hybrid Nanogenerators for Wearable Self-Powered Systems and Active Remote Sensing', ACS Appl Mater Interfaces, vol. 10, no. 17, pp. 14708–14715, May 2018, doi: 10.1021/acsami.8b01635.

[11] Q. Zhou, J. Pan, S. Deng, F. Xia, and T. Kim, 'Triboelectric Nanogenerator-Based Sensor Systems for Chemical or Biological Detection', Sep. 01, 2021, John Wiley and Sons Inc. doi: 10.1002/adma.202008276.

[12] [Y. Hao, Y. Zhang, A. Mensah, S. Liao, P. Lv, and Q. Wei, 'Scalable, ultra-high stretchable and conductive fiber triboelectric nanogenerator for biomechanical sensing', Nano Energy, vol. 109, May 2023, doi: 10.1016/j.nanoen.2023.108291.

[13] Y. Zou et al., 'A flexible self-arched biosensor based on combination of piezoelectric and triboelectric effects', Appl Mater Today, vol. 20, Sep. 2020, doi: 10.1016/j.apmt.2020.100699.

[14] X. Pu, C. Zhang, and Z. L. Wang, 'Triboelectric nanogenerators as wearable power sources and self-powered sensors', Jan. 01, 2023, Oxford University Press. doi: 10.1093/nsr/nwac170.

[15] H. Guo et al., 'A highly sensitive, self-powered triboelectric auditory sensor for social robotics and hearing aids', Sci Robot, vol. 3, no. 20, 2018, [Online]. Available: http://robotics.sciencemag.org/

[16] L. Liu et al., 'Ultra-high output hybrid nanogenerator for self-powered smart mariculture monitoring and warning system', Chemical Engineering Journal, vol. 472, Sep. 2023, doi: 10.1016/j.cej.2023.145039.

[17] Z. L. Wang, T. Jiang, and L. Xu, 'Toward the blue energy dream by triboelectric nanogenerator networks', Sep. 01, 2017, Elsevier Ltd. doi: 10.1016/j.nanoen.2017.06.035.

[18] X. Wei et al., 'All-Weather Droplet-Based Triboelectric Nanogenerator for Wave Energy Harvesting', ACS Nano, vol. 15, no. 8, pp. 13200–13208, Aug. 2021, doi: 10.1021/acsnano.1c02790.

[19] C. Zhang et al., 'Active resonance triboelectric nanogenerator for harvesting omnidirectional water-wave energy', Joule, vol. 5, no. 6, pp. 1613–1623, Jun. 2021, doi: 10.1016/j.joule.2021.04.016.

[20] F. Jean, M. U. Khan, A. Alazzam, and B. Mohammad, 'Harnessing ambient sound: Different approaches to acoustic energy harvesting using triboelectric nanogenerators', Dec. 01, 2024, Elsevier B.V. doi: 10.1016/j.jsamd.2024.100805.

[21] S. R. Patil et al., 'Triboelectric Nanogenerator Based on Biowaste Tribopositive Delonix Regia Flowers Powder', Energy Technology, vol. 10, no. 12, Dec. 2022, doi: 10.1002/ente.202200876.

[22] S. A. Lone et al., 'Recent advancements for improving the performance of triboelectric nanogenerator devices', Nano Energy, vol. 99, Aug. 2022, doi: 10.1016/j.nanoen.2022.107318.

[23] F. F. Hatta, M. A. S. Mohammad Haniff, and M. A. Mohamed, 'A review on applications of graphene in triboelectric nanogenerators', Feb. 01, 2022, John Wiley and Sons Ltd. doi: 10.1002/er.7245.

[24] H. Sun et al., 'Graphene-based dual-function acoustic transducers for machine learning-assisted human–robot interfaces', InfoMat, vol. 5, no. 2, Feb. 2023, doi: 10.1002/inf2.12385.

[25] D. Zhang, Z. Xu, Z. Yang, and X. Song, 'High-performance flexible self-powered tin disulfide nanoflowers/reduced graphene oxide nanohybrid-based humidity sensor driven by triboelectric nanogenerator', Nano Energy, vol. 67, Jan. 2020, doi: 10.1016/j.nanoen.2019.104251.

[26] W. Sun, G. Ji, J. Chen, D. Sui, J. Zhou, and J. Huber, 'Enhancing the acoustic-to-electrical conversion efficiency of nanofibrous membrane-based triboelectric nanogenerators by nanocomposite composition', Nano Energy, vol. 108, Apr. 2023, doi: 10.1016/j.nanoen.2023.108248.

[27] Y. Zhou, W. Deng, J. Xu, and J. Chen, 'Engineering Materials at the Nanoscale for Triboelectric Nanogenerators', Aug. 26, 2020, Cell Press. doi: 10.1016/j.xcrp.2020.100142.

[28] D. Deepak, N. Soin, and S. S. Roy, 'Optimizing the efficiency of triboelectric nanogenerators by surface nanoarchitectonics of graphene-based electrodes: A review', Mar. 01, 2023, Elsevier Ltd. doi: 10.1016/j.mtcomm.2023.105412.

[29] W. T. Guo et al., 'Printed-scalable microstructure BaTiO3/ecoflex nanocomposite for high-performance triboelectric nanogenerators and self-powered human-machine interaction', Nano Energy, vol. 131, Dec. 2024, doi: 10.1016/j.nanoen.2024.110324.

[30] S. Zhou et al., 'Recent advances in TENGs collecting acoustic energy: From low-frequency sound to ultrasound', Oct. 01, 2024, Elsevier Ltd. doi: 10.1016/j.nanoen.2024.109951.

[31] M. Yuan et al., 'Integrated acoustic metamaterial triboelectric nanogenerator for joint low-frequency acoustic insulation and energy harvesting', Nano Energy, vol. 122, Apr. 2024, doi: 10.1016/j.nanoen.2024.109328.

[32] M. Shanbedi, H. Ardebili, and A. Karim, 'Polymer-based triboelectric nanogenerators: Materials, characterization, and applications', Sep. 01, 2023, Elsevier Ltd. doi: 10.1016/j.progpolymsci.2023.101723.

[33] Y. Mi, Z. Zhao, H. Wu, Y. Lu, and N. Wang, 'Porous Polymer Materials in Triboelectric Nanogenerators: A Review', Nov. 01, 2023, Multidisciplinary Digital Publishing Institute (MDPI). doi: 10.3390/polym15224383.

[34] Y. Mi et al., 'Biodegradable Polymers in Triboelectric Nanogenerators', Jan. 01, 2023, MDPI. doi: 10.3390/polym15010222.

[35] X. Suo et al., 'Dielectric layer doping for enhanced triboelectric nanogenerators', Sep. 01, 2023, Elsevier Ltd. doi: 10.1016/j.nanoen.2023.108651.

[36] M. Yuan et al., 'Triboelectric nanogenerator metamaterials for joint structural vibration mitigation and self-powered structure monitoring', Nano Energy, vol. 103, Dec. 2022, doi: 10.1016/j.nanoen.2022.107773.

[37] H. Zhang, L. Wang, C. Zhang, J. Shu, K. Huang, and Y. Song, 'A general modification of the V-Q-x relationship of the contact-separation mode triboelectric nanogenerator', Nano Energy, vol. 115, Oct. 2023, doi: 10.1016/j.nanoen.2023.108716.

[38] X. Xiao et al., 'Research on an Optimized Quarter-Wavelength Resonator-Based Triboelectric Nanogenerator for Efficient Low-Frequency Acoustic Energy Harvesting', Nanomaterials, vol. 13, no. 10, May 2023, doi: 10.3390/nano13101676.

[39] R. Zhang and H. Olin, 'Material choices for triboelectric nanogenerators: A critical review',

EcoMat, vol. 2, no. 4, Dec. 2020, doi: 10.1002/eom2.12062.
[40] Z. L. Wang, L. Lin, J. Chen, S. Niu, and Y. Zi, Triboelectric Nanogenerators. Cham: Springer International Publishing, 2016. doi: 10.1007/978-3-319-40039-6.
[41] H. Zou et al., 'Quantifying the triboelectric series', Nat Commun, vol. 10, no. 1, Dec. 2019, doi: 10.1038/s41467-019-09461-x.
[42] L. Zhang, Y. Liu, X. Sun, and Z. Wen, 'Advances in triboelectric nanogenerators in acoustics: Energy harvesting and Sound sensing', Nano Trends, vol. 8, p. 100064, Dec. 2024, doi: 10.1016/j.nwnano.2024.100064.
[43] A. Chen, C. Zhang, G. Zhu, and Z. L. Wang, 'Polymer Materials for High-Performance Triboelectric Nanogenerators', Jul. 01, 2020, John Wiley and Sons Inc. doi: 10.1002/advs.202000186.
[44] F. Ali et al., 'Triboelectric Nanogenerator Based on PTFE Plastic Waste Bottle and Aluminum Foil', Materials Innovations, vol. 2, no. 8, pp. 203–213, Aug. 2022, doi: 10.54738/mi.2022.2803.
[45] P. Ravi Sankar, P. Supraja, S. Mishra, K. Prakash, R. Rakesh Kumar, and D. Haranath, 'A novel triboelectric nanogenerator based on only food packaging aluminium foils', Mater Lett, vol. 310, Mar. 2022, doi: 10.1016/j.matlet.2021.131474.
[46] A. Pratap et al., 'Direct writing of PVBVA/Ti3C2 Tx (MXene) triboelectric nanogenerators for energy harvesting and sensing applications', Nano Energy, vol. 142, Sep. 2025, doi: 10.1016/j.nanoen.2025.111206.
[47] Y. J. Kim, J. Lee, S. Park, C. Park, C. Park, and H. J. Choi, 'Effect of the relative permittivity of oxides on the performance of triboelectric nanogenerators', RSC Adv, vol. 7, no. 78, pp. 49368–49373, 2017, doi: 10.1039/c7ra07274k.
[48] G. Khandelwal, N. P. Maria Joseph Raj, and S. J. Kim, 'Materials Beyond Conventional Triboelectric Series for Fabrication and Applications of Triboelectric Nanogenerators', Sep. 01, 2021, John Wiley and Sons Inc. doi: 10.1002/aenm.202101170.
[49] Z. Liu et al., 'Crystallization-Induced Shift in a Triboelectric Series and even Polarity Reversal for Elastic Triboelectric Materials', Nano Lett, vol. 22, no. 10, pp. 4074–4082, May 2022, doi: 10.1021/acs.nanolett.2c00767.
[50] L. Wang, Y. Dong, J. Tao, T. Ma, and Z. Dai, 'Study of the mechanisms of contact electrification and charge transfer between polytetrafluoroethylene and metals', J Phys D Appl Phys, vol. 53, no. 28, Jul. 2020, doi: 10.1088/1361-6463/ab813e.
[51] J. ho Son et al., 'Recycled, Contaminated, Crumpled Aluminum Foil-Driven Triboelectric Nanogenerator', Advanced Science, vol. 10, no. 28, Oct. 2023, doi: 10.1002/advs.202301609.
[52] B. Xie et al., 'Advances in Graphene-Based Electrode for Triboelectric Nanogenerator', Dec. 01, 2025, Springer Science and Business Media B.V. doi: 10.1007/s40820-024-01530-1.
[53] S. M. M. Shoumik, M. H. Shahriar, M. M. Hossain, F. M. Nizazul Islam, B. B. Saha, and S. Ghosh, 'Enhancement of Aluminum Polytetrafluoroethylene Based Triboelectric Nanogenerator for High Temperature Environment', in 2024 International Conference on Innovations in Science, Engineering and Technology: Innovative Technologies for Global Solutions, ICISET 2024, Institute of Electrical and Electronics Engineers Inc., 2024. doi: 10.1109/ICISET62123.2024.10939170.
[54] Z. Zhao et al., 'Selection rules of triboelectric materials for direct-current triboelectric nanogenerator', Nat Commun, vol. 12, no. 1, Dec. 2021, doi: 10.1038/s41467-021-25046-z.
[55] [W. A. Brainard and D. H. Buckley, 'Adhesion and friction of PTFE in contact with metals as studied by auger spectroscopy, field ion and scanning electron microscopy', Elsevier Sequoia S.A, 1973.
[56] K. Wang et al., 'Triboelectric nanogenerator module for circuit design and simulation', Nano Energy, vol. 107, Mar. 2023, doi: 10.1016/j.nanoen.2022.108139.
[57] D. Zhao et al., 'Universal equivalent circuit model and verification of current source for triboelectric nanogenerator', Nano Energy, vol. 89, Nov. 2021, doi: 10.1016/j.nanoen.2021.106335.

Correction/ Revision Table

	Comments	Sentences/Example	Issue	Suggestion	Correction/revision
1.	Language and Grammar (Page 2, Abstract & Introduction)	"(PTFE) and Aluminium was selected to be the triboelectric materials…"	Subject–verb agreement ("was" → "were").	Revise for grammar consistency. Example: "PTFE and Aluminium were selected as the triboelectric materials…"	The word "was" replaced with "were"
2.	Clarity of Equations (Page 4, Equations 1–5)	-	Several variables (e.g., σ, ε_0, x) are introduced without immediate definition in the text.	Provide explicit definitions for all variables when equations are presented, and ensure uniform formatting (e.g., italicized symbols).	Better explicit definitions were provided immediately after its corresponding equation and formatting was fixed
3.	Reference Formatting (Throughout, esp.	Example: "Triboelectric Nanogenerator or	Reference numbers sometimes appear	Standardize citation style according to IJNeaM	Better explicit definitions was provided immediately

	Pages 2–3, 9–11)	(TENG) is an emerging technology…" [1], [2].	with inconsistent spacing.	guidelines (e.g., [1,2] instead of [1], [2]).	after its corresponding equation and formatting was fixed
4.	Figures Captions (Page 5, Figures 3 & 4)	Caption: "PTFE film and Aluminium film/foil used in the TENG"	Captions are too brief and lack experimental context.	Expand captions to include key parameters (thickness, diameter, preparation details). For example: "PTFE film (0.5 mm, 80 mm diameter) and Aluminium foil used as triboelectric layers in the TENG."	Captions were expanded by providing more context to the figure.
5.	Novelty Limitation (Results & Discussion)		The paper reports that similar PTFE–Al TENGs in literature have produced much higher voltages (up to 1400 V [44]), while this study only achieved 2.36 V. The authors acknowledge this gap but do not sufficiently justify or propose how their work adds unique value.	Include a comparison table of PTFE–Al TENG outputs from recent literature (2022–2025) versus this study, and highlight what makes this design distinct (e.g., low-cost approach, simple fabrication, use in acoustic chamber). Emphasize novelty more clearly.	More discussion and a comparison table were added.
6.	Surface Interaction and Poor Separation (Figure 9 & Discussion)		The observation that "the triboelectric layers stick and oscillate together instead of separating" is plausible, but it is not supported by additional experiments. This weakens the argument that adhesion is the main cause of poor performance.	: Conduct surface characterization (SEM imaging, surface roughness analysis, or contact angle tests) to verify the adhesion issue. Alternatively, discuss possible design modifications such as surface texturing, nano-coatings, or adding an intermediate polymer layer to improve separation.	The suggestion of adding an intermediate layer was added and discussed in this study.
7.	Limited Practical Insights from Resistive Loading (Page 6, Resistive Loading Analysis)		The study reports that the maximum power output is 0.206 μW at 7 MΩ, but the discussion ends without linking this to practical use. Readers are left uncertain about the relevance of this output.	Compare the achieved power level with typical requirements of low-power applications (e.g., IoT sensors, microphones, or wearable devices). This would help demonstrate whether the design is moving toward practical viability or requires scaling/improvement.	The achieved power of the TENG was compared to the power level of small electronic devices such as LEDs.
8.	Conclusion Too General (Page 6)		The statement "a better design that could allow proper contact and separation process need to be implemented" is too broad and does not provide concrete guidance for future work.	Strengthen the conclusion with specific recommendations, such as: Introducing nano/micro structuring on PTFE surface to reduce adhesion. Exploring hybrid materials (PTFE combined with graphene oxide, PVDF, or PDMS). Modifying acoustic chamber	More recommendation was added to the conclusion according to the suggestion of this issue

				geometry to enhance vibration energy transfer. Testing alternative electrode metals with lower adhesion to PTFE.	